IUE Final Archive Calibration: LWP and SWP High-Dispersion Resolution Analysis

Matthew P. Garhart and Corinne M. Eby
Computer Sciences Corporation
10000-A Aerospace Road
Lanham-Seabrook, Maryland 20706
Electronic-mail: calib@gorgon.gsfc.nasa.gov

01 July 1996

Introduction

The instrumental resolution (both spectral and spatial) is a convolution of the camera resolution, dispersion mode, spectrograph entrance aperture, telescope focus, and spacecraft pointing stability. While the dominant effect is due to the camera, telescope focus and spacecraft pointing stability also play a major role in defining the resolution. In addition, it is well known that the camera resolution is highly wavelength dependent. According to the *IUE* Camera Users Guide (Coleman *et al.* 1977), the camera point spread function (PSF) consists of a narrow gaussian-like core having a full width at half maximum (FWHM) of 2 to 5 pixels and a weak long-range tail. The actual resolution in either the spatial or spectral direction can be defined as a function of the FWHM. The Rayleigh criterion of instrumental resolution specifies that two spectra (spatial direction) or two spectral features (spectral direction) can be resolved provided their separation is as follows (Weinstein and Pérez 1992):

$$d \geq 0.849 \times FWHM$$

where d is the distance separating the two features (or spectra). The gaussian fitting routine used in this analysis was GAUSSFITS, taken from the *IUE* Data Analysis Center software library. This procedure outputs the one-sigma width of the fitted gaussian profile which was then converted to FWHM using the statistical equality (Bevington 1969):

$$FWHM = 2.3548 \times \sigma$$

Resolution Perpendicular to the Dispersion

The spatial resolution has been determined by analyzing the spectra of high-dispersion standard stars. The FWHM of several pairs of large and small-aperture line-by-line images were measured at five sample positions (*viz.*, 134, 258, 384, 507, and 615). For each sample position, a three pixel wide average cross-cut perpendicular to the dispersion was taken and the widths of the orders measured using the gaussian fitting routine. The results for each image were in good agreement, so we averaged the results to yield a set of spectral widths for each aperture as a function of order

number and sample position. The differences in telescope focus between the images were kept small so as to minimize the effect of focus on the resolution measurements (Pérez *et al.* 1990). The spatial resolution data and the one-sigma error bars for each sample position are plotted as a function of order number. The small-aperture data are horizontally offset to the left of the large-aperture data by half an order for clarity. A seventh-order polynomial fit to the data is also provided.

LWP

LWP spatial resolution images are listed in Table 1 and the FWHM measurements are plotted in Figures 1–5. The database contains a combination of optimally exposed images for the central orders and overexposed (in the central orders only) images for the extreme orders. The spatial resolution for sample position 384 is approximately 3.5 pixels FWHM at order 69 and decreases to 2.3 pixels at order 80 where it is roughly constant for the remaining orders. The spatial resolution degrades as one moves towards smaller sample positions and improves slightly (as compared with sample position 384) above order 90 for sample position 507. Small-aperture resolution shows an average improvement (over all orders and sample positions) of 5% over the large aperture. This difference is most apparent between orders 80 through 100 and at the smaller sample positions where it is as much as 8% for sample position 134.

Unfortunately, no LWP high-dispersion spatial resolution studies could be found for IUESIPS data.

SWP

Table 2 lists the images used for the SWP spatial resolution analysis and the FWHM data are plotted in Figures 6–10. The resolution trends as a function of order number are, in general, the same for every sample position. The FWHM is around 4 pixels at order 66 (long wavelengths) and decreases to approximately 2 pixels near order 100 (short wavelengths). Unlike the indications from previous IUESIPS studies (*e.g.*, Bianchi (1980), Schiffer (1980), and Cassatella *et al.* (1981)), this decrease is not linear with order number. A plateau of around 3.0 pixels FWHM occurs between orders 75 and 85. This trend is confirmed by the analysis of de Boer *et al.* (1983) which displayed the order widths using 2-D contour plots. The FWHM remains fairly constant for the remaining orders of sample positions 258 and 384. At these sample positions, the higher orders (100 and above) are well away from the edge of the camera. The more extreme sample positions (*i.e.*, 134 and 615) show an edge effect as the resolution dramatically worsens above order 100. The best spatial resolution occurs near sample position 384 and worsens slightly as one moves towards smaller sample positions (*i.e.*, shorter wavelengths within an order). Differences in resolution between the large and small apertures are small. The small aperture shows an average improvement (over all orders) of 2.7% in resolution over the large aperture.

As is the case with the low-dispersion resolution studies, the NEWSIPS values show an improvement over IUESIPS measurements. Schiffer (1980) quoted FWHM values of 3.5 pixels for order 75 and 2.4 pixels for order 105. The NEWSIPS results for those orders are 3.3 pixels and 2.1 pixels, respectively. Analysis by de Boer *et al.* (1983) showed the best resolution of 2.4 pixels FWHM occuring near the center of the camera. The NEWSIPS results indicate a FWHM of 2.0 pixels in this same area (sample position 384). Also, Bianchi (1980) expressed FWHM as a function of order number, regardless of camera, according to the following formula: $FWHM = 7.23 - 0.04 \times m$ where m is order number and the FWHM is in pixels. Thus, for order 71, this indicates a FWHM of 4.4 pixels, a figure that is almost 20% higher than our average measurement for that order.

Resolution Along the Dispersion

A study of the spectral resolution was performed utilizing several methods. The first measured emission lines from small-aperture wavelength calibration (WAVECAL) images obtained using the on-board hollow cathode platinum-neon (Pt-Ne) calibration lamp. The second measured several features from the emission line sources V1016 Cyg and RR Tel and interstellar absorption line features from the calibration standard BD+75° 325. The third method measured absorption features from the calibration standard HD 149757 (Zeta Oph). The WAVECAL images are useful in determining the spectral resolution as they are not affected by the telescope focus nor are they subject to astrophysical broadening. The Zeta Oph spectra are characterized by very narrow interstellar absorption features so they are also useful for measuring spectral resolution. Therefore, the measurements taken from WAVECAL and Zeta Oph images represent the best possible spectral resolution obtainable.

LWP

The WAVECAL and large-aperture Zeta Oph resolution data are displayed in Figures 11 and 13, respectively. The results, along with the associated one-sigma error bars and linear fits (dashed line), are plotted as a function of order number in both wavelength and pixel space. The dotted line in the pixel space plots is the average of the resolution data over all orders. No small-aperture high-dispersion data of Zeta Oph is available. In addition, the standard star, RR Tel, and V1016 Cyg data were too noisy to yield suitable results. The large-aperture Zeta Oph measurements are quite similar to the small-aperture WAVECAL analysis. The spectral resolution in wavelength space is approximately 0.18Å FWHM at order 75 and linearly decreases (roughly) to 0.11Å at order 117. The pixel space data for both WAVECALs and Zeta Oph show the same improvement in resolution between orders 95 and 110. The *IUE* Systems Design Report (GSFC 1976) lists 15,000 ($\lambda/\Delta\lambda$) as the high-dispersion resolution for the long-wavelength cameras. This yields 0.22Å for order 69, 0.17Å for order 90, and 0.13Å for order 123. These numbers are comparable to our results of

0.24Å, 0.15Å, and 0.12Åfor these same orders.

The only report which discussed LWP high-dispersion spectral resolution was by Evans and Imhoff (1985). They measured the FWHM of emission lines obtained from WAVECAL images and processed through IUESIPS software. The results are as follows: 0.22Å for order 75, 0.17Å for order 83, 0.13Å for order 96, and 0.13Å for order 116. These figures are very similar to our results of 0.20Å, 0.14Å, 0.15Å, and 0.13Å.

SWP

The WAVECAL, Zeta Oph, and large- and small-aperture stellar source spectral resolution data are displayed in Figures 12, 14, 15, and 16. As is the case with the LWP, the plots include one-sigma error bars and linear (dashed line) and mean (dotted line) fits to the data. In Figures 15 and 16, the emission line measurements for orders 111 and above were excluded from the analysis when performing the linear fit to the stellar data. The spectral resolution in wavelength space for the WAVECAL, Zeta Oph, and stellar source images shows no dependence on wavelength within an order and a roughly linear dependence on order number. Unlike the LWP, the SWP resolution from the Zeta Oph analysis (Figure 14) is much worse than the corresponding WAVECAL data (Figure 12). The stellar source results are somewhat inconclusive for orders 111 and above. The emission line widths are dramatically higher than the corresponding absorption line measurements. This trend was also seen in the analysis by Grady (1985). The *IUE* Systems Design Report (GSFC 1976) quotes a figure of 10,000 ($\lambda/\Delta\lambda$) for the spectral resolution in high-dispersion mode. This corresponds to a FWHM of approximately 0.2Å for order 66 and 0.1Å for order 125. This same trend is seen in the top plot (Figure 12) of the WAVECAL resolution analysis. The fact that the spectral resolution is a constant value is verified by the pixel space results (bottom plot) that show little dependence on order. The stellar source resolution measurements in pixel space (bottom plot of Figures 15 and 16) show some degradation towards higher order numbers. In addition, the small-aperture data (Figure 16) indicates an 8% improvement in resolution over the large-aperture counterpart (Figure 16).

The general trend of the wavelength-space resolution for the WAVECAL images is approximately the same for every IUESIPS study that has been reviewed (*i.e.*, Boggess *et al.* 1978, Cassatella *et al.* 1981, Cassatella and Martin 1982, and Evans and Imhoff 1985). That is, the camera resolution in wavelength space varies roughly linearly with order number and improves towards shorter wavelengths (0.19Å for order 69 and 0.09Å for order 106). The results from our analysis of WAVECAL images processed through NEWSIPS are almost identical to these figures. Penston (1979) reported SWP large-aperture FWHM values of 0.20Å for absorption lines and 0.24Å

for emission lines. These figures are comparable with our average results of 0.21Å and 0.23Å respectively. However, Penston's (1979) measurements for the small-aperture resolution are no better than the large aperture. This result could be supported by our study as the apparent improvement in small-aperture resolution is less than the one-sigma error of the FWHM average for any given order. Grady (1985) assessed the effects of the two-gyro control mode on high-dispersion data using large-aperture RR Tel spectra. The mean resolution (averaged over all orders) from her analysis (0.22Å) agrees with our average resolution result.

Conclusions

In general, the small aperture yields a slight increase in resolution over the large aperture. The NEWSIPS spatial resolution data show an improvement over IUESIPS. The NEWSIPS spectral resolution results, on the other hand, demonstrate similar resolution compared to data processed with IUESIPS.

References

Bevington, P.R. 1969, Data Reduction and Error Analysis for the Physical Sciences (New York, McGraw-Hill)

Bianchi, L. 1980, in IUE Data Reduction, edited by W.W. Weiss *et al.*(Austrian Solar and Space Agency, Vienna), pp. 161–166

Boggess, A., Bohlin, R.C., Evans, D.C., Freeman, H.R., Gull, T.R., Heap, S.R., Klinglesmith, D.A., Longanecker, G.R., Sparks, W., West, D.K., Holm, A.V., Perry, P.M., Schiffer, F.H., Turnrose, B.E., Wu, C.C., Lane, A.L., Linsky, J.L., Savage, B.D., Benvenuti, P., Cassatella, A., Clavel, J., Heck, A., Macchetto, F., Penston, M.V., Selvelli, P.L., Dunford, E., Gondhalekar, P., Oliver, M.B., Sanford, M.C.W., Stickland, D., Bokensberg, A., Coleman, C.I., Snijders, M.A.J., Wilson, R. 1978, Nature, 275, 377

Cassatella, A., Martin, T., and Ponz D., *Report to the IUE Three-Agency Coordination Meeting*, October 1981

Cassatella, A. and Martin, T., *Report to the IUE Three-Agency Coordination Meeting*, September 1982

Coleman, C., Golton, E., Gondhalekar, P., Hall, J., Oliver, M., Sanford, M., Snijders, T., and Stewart, B. 1977, *IUE Technical Note No. 31, Camera Users Guide*, UK Camera Operations Group Issue 1, October 1977, Appleton Laboratory, University College London

de Boer, K.S., Preussner, P.R., and Grewing, M. 1983, IUE NASA Newsletter, No. 20, 15

Evans, N.R. and Imhoff, C.L. 1985, IUE NASA Newsletter, No. 28, 77
Grady, C.A., *Record of the IUE Three-Agency Coordination Meeting*, October 1985
Goddard Space Flight Center, *System Design Report for the International Ultraviolet Explorer*, IUE-401-76-099, August 1976
Penston, M., *Report to the IUE Three-Agency Coordination Meeting*, March 1979
Pérez, M.R., Huber, L.F., and Esper, J. 1990, IUE NASA Newsletter, No. 45, 31
Schiffer, F.H., *Report to the IUE Three-Agency Coordination Meeting*, November 1980
Weinstein, D. and Pérez, M.R. 1992, *Record of the IUE Three-Agency Coordination Meeting*, November 1992

Table 1: LWP High-Dispersion Spatial Resolution Images

Object Name	Image Number	Date (Yr/Day)	THDA	Focus	Aperture	Exposure Level
HD 149438	1965	83/206	10.5	−2.2	Large	Optimal
	3155	84/105	10.5	−2.5	Large	Optimal
	3690	84/183	8.2	−1.4	Large	Optimal
	8559	86/188	9.5	−2.7	Large	Optimal
	10132	87/047	9.8	−2.2	Large	Optimal
	11422	87/230	9.5	−2.2	Large	Optimal
	13679	88/199	9.8	−2.3	Large	4X over
	13690	88/200	9.8	−2.3	Large	4X over
	13732	88/206	9.8	−2.8	Large	4X over
	13735	88/206	10.2	−3.6	Large	4X over
	31526	95/266	8.5	−9.4	Large	Optimal
	1979	83/231	11.2	−3.0	Small	Optimal
	2725	84/032	9.5	−1.1	Small	Optimal
	3691	84/183	8.5	−1.6	Small	Optimal
	8565	86/189	10.2	−2.1	Small	Optimal
	10309	87/069	8.8	−1.4	Small	Optimal
	11423	87/230	8.8	−3.7	Small	Optimal
	31525	95/266	7.8	−6.7	Small	Optimal
	31527	95/266	8.5	−11.3	Small	8X over
HD 120315	6317	85/182	9.5	−2.9	Large	Optimal
	7650	86/042	7.8	−2.8	Large	Optimal
	13693	88/200	10.2	−2.8	Large	4X over
	13696	88/200	10.8	−0.9	Large	4X over
	13705	88/202	11.5	−2.2	Large	4X over
	6387	85/194	7.5	−2.3	Small	Optimal
	7415	85/364	11.8	−2.3	Small	Optimal
HD 207198	6018	85/141	9.5	−2.1	Large	Optimal
	6066	85/146	11.8	−2.9	Small	Optimal

Table 2: SWP High-Dispersion Spatial Resolution Images

Object Name	Image Number	Date (Yr/Day)	THDA	Focus	Aperture
HD 3360	7807	80/029	8.5	−0.5	Large
	23376	84/183	8.2	−3.1	Large
	7806	80/029	8.2	−0.8	Small
	23862	84/247	6.8	−3.2	Small
HD 120315	9549	80/202	5.8	−2.2	Large
	25548	85/089	10.8	−2.7	Large
	9069	80/142	7.8	−1.5	Small
	25565	85/092	8.5	−1.4	Small
HD 149438	26512	85/212	9.2	−2.3	Large
	28628	86/188	9.5	−3.0	Large
	30317	87/047	9.5	−2.2	Large
	31581	87/230	9.2	−2.2	Large
	30474	87/069	7.8	−1.1	Small
	26534	85/215	8.8	−2.7	Small
	28634	86/189	8.8	−2.3	Small
	31582	87/230	8.8	−2.9	Small

Table 3: LWP High-Dispersion Spectral Resolution Images

Object Name	Image Number	Date (Yr/Day)	THDA	Focus	Aperture
WAVECAL	1221	80/168	7.2	−2.7	Small
	2010	83/274	12.2	−1.5	Small
	7911	86/089	9.2	−0.4	Small
	15419	89/120	8.5	−1.3	Small
	15420	89/120	8.8	−1.6	Small
	16042	89/213	10.2	−2.1	Small
	24042	92/275	13.2	−4.2	Small
	30581	95/120	8.5	−2.5	Small
Zeta Oph	13114	88/114	8.8	−2.7	Large
	17574	90/081	11.2	−1.5	Large
	19991	91/085	11.8	−1.7	Large
	23462	92/189	9.8	+0.3	Large

Table 4: SWP High-Dispersion Spectral Resolution Images

Object Name	Image Number	Date (Yr/Day)	THDA	Focus	Aperture
WAVECAL	4603	79/071	15.9	+5.2	Small
	17191	82/162	9.2	−1.0	Small
	26652	85/251	5.8	+0.2	Small
	33023	88/062	11.8	−0.6	Small
	37999	90/013	6.8	−2.8	Small
	38000	90/013	6.8	−2.0	Small
	44276	92/091	6.1	−3.3	Small
	55173	95/171	8.8	−4.4	Small
RR Tel	2247	78/220	9.5	+1.2	Large
	3407	78/325			Large
	10434	80/294	9.2	−1.2	Large
	14230	81/160	8.5	+0.6	Large
	14729	81/223	12.5	−0.8	Large
	15229	81/283	9.2	−0.9	Large
	20246	83/168	11.8	−1.3	Large
	28740	86/205	6.5	−3.2	Large
	28741	86/205	6.8	−1.7	Large
	28745	86/206	9.5	−0.3	Large
	4432	79/059		−1.2	Small
	14229	81/160	8.5	−0.1	Small
	15210	81/281	9.8	−1.1	Small
	28808	86/213	7.8	−1.9	Small

Table 4 (cont.): SWP High-Dispersion Spectral Resolution Images

Object Name	Image Number	Date (Yr/Day)	THDA	Focus	Aperture
V1016 Cyg	16746	82/101	11.5	−1.3	Large
	1669	78/150		+1.9	Small
	2425	78/243		+0.1	Small
	2426	78/243		+0.6	Small
	16700	82/096	7.8	−1.6	Small
BD+75°325	34254	88/259	9.8	−2.4	Large
	35152	88/362	6.5	−1.1	Large
	35153	88/362	6.8	−1.8	Large
	35351	89/015	8.2	−1.8	Large
	35405	89/025	9.2	−2.6	Large
	35459	89/030	7.8	−2.0	Large
	3325	78/317	8.8	−0.6	Small
	3326	78/317	8.8	+0.1	Small
	3710	78/360	8.5	−0.4	Small
Zeta Oph	14428	81/190	12.8	+1.0	Large
	16493	82/069	5.5	−0.5	Large
	17918	82/254	8.2	−0.6	Large
	18125	82/270	9.5	−0.6	Large
	19430	83/069	9.2	−1.2	Large
	41190	91/085	12.2	−2.6	Large
	1784	78/165	6.1	−0.8	Small
	2905	78/283	7.8	−0.3	Small
	2906	78/284	7.8	−0.7	Small
	5934	79/205	7.2	−1.3	Small
	9690	80/216	7.8	−1.5	Small
	9808	80/229	9.8	−1.0	Small

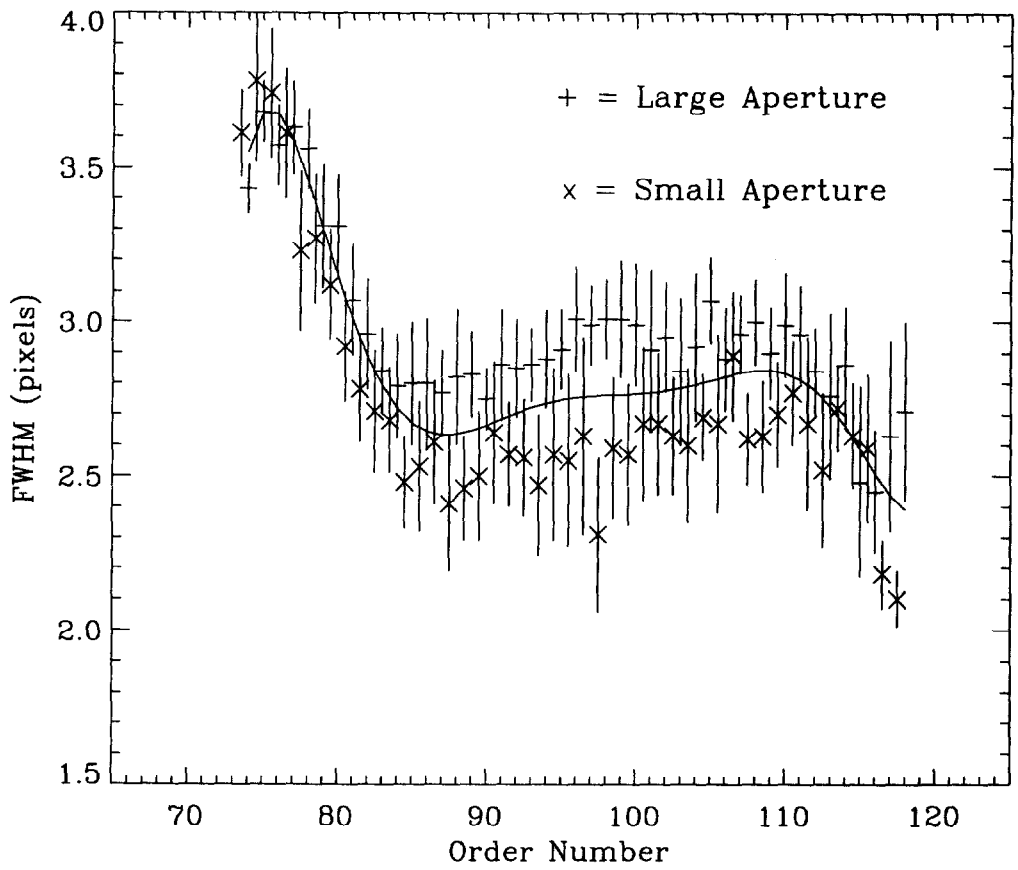

Figure 1: LWP high-dispersion spatial resolution for sample position 134. Small-aperture data is horizontally offset to the left of the large-aperture data by half an order.

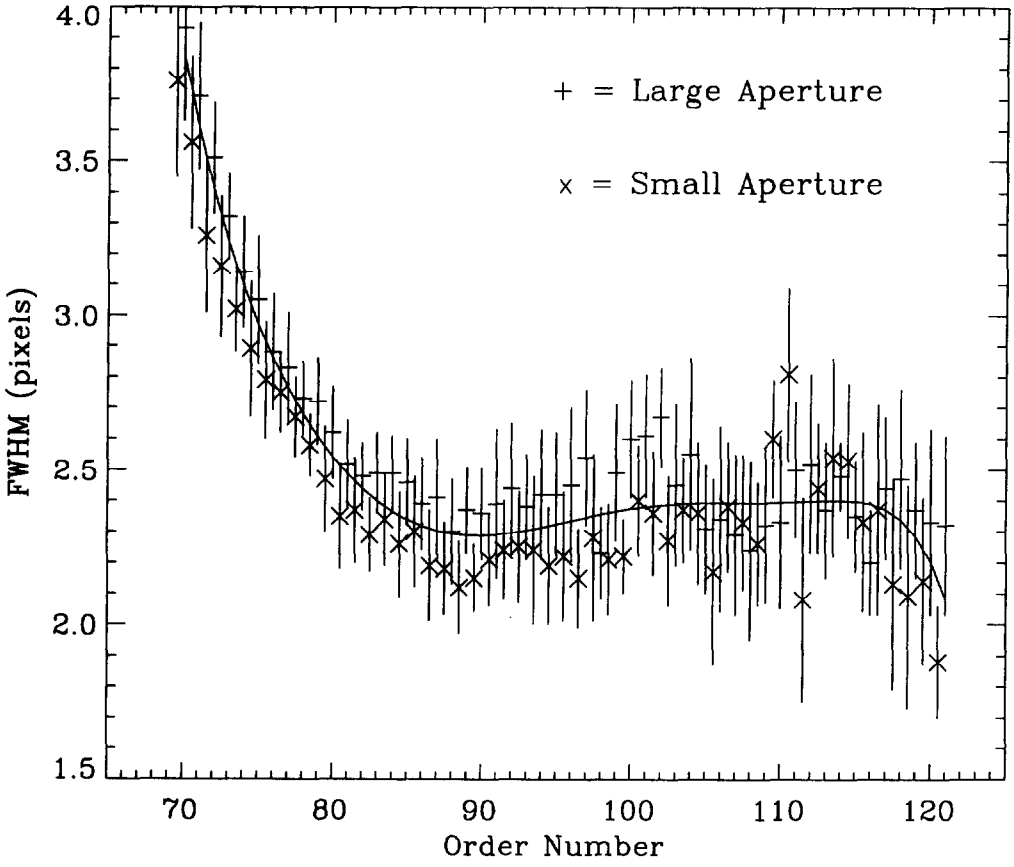

Figure 2: LWP high-dispersion spatial resolution for sample position 258. Small-aperture data is horizontally offset to the left of the large-aperture data by half an order.

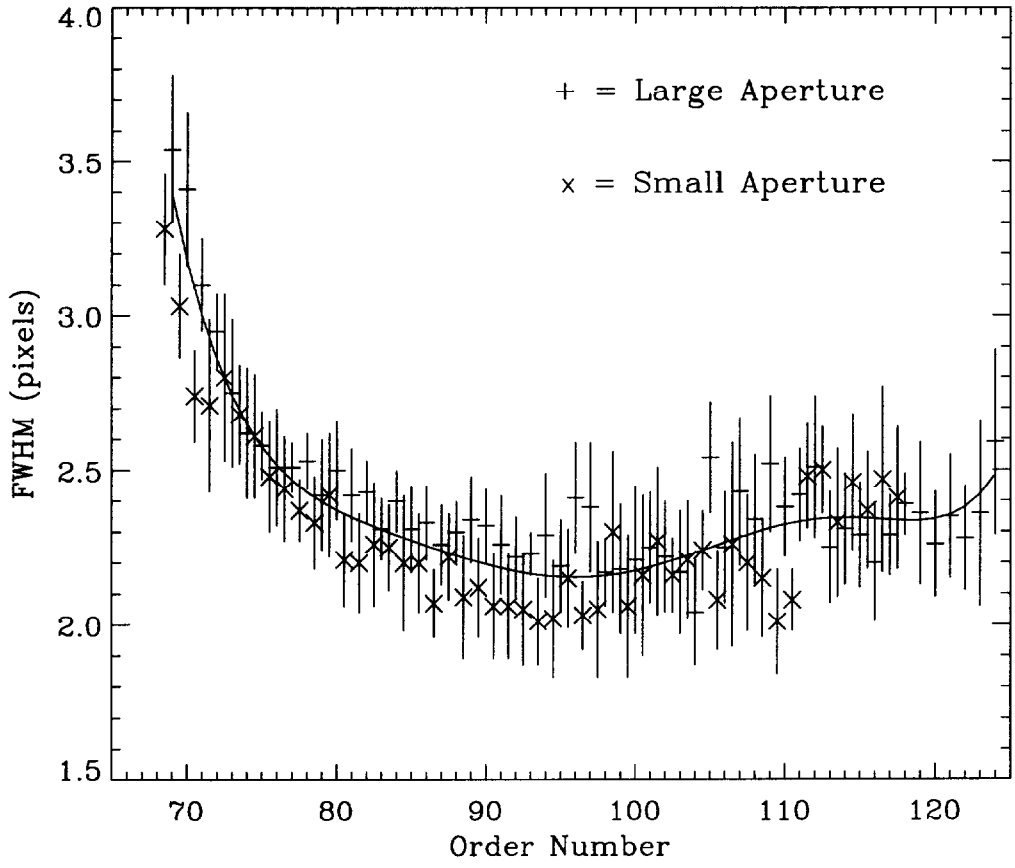

Figure 3: LWP high-dispersion spatial resolution for sample position 384. Small-aperture data is horizontally offset to the left of the large-aperture data by half an order.

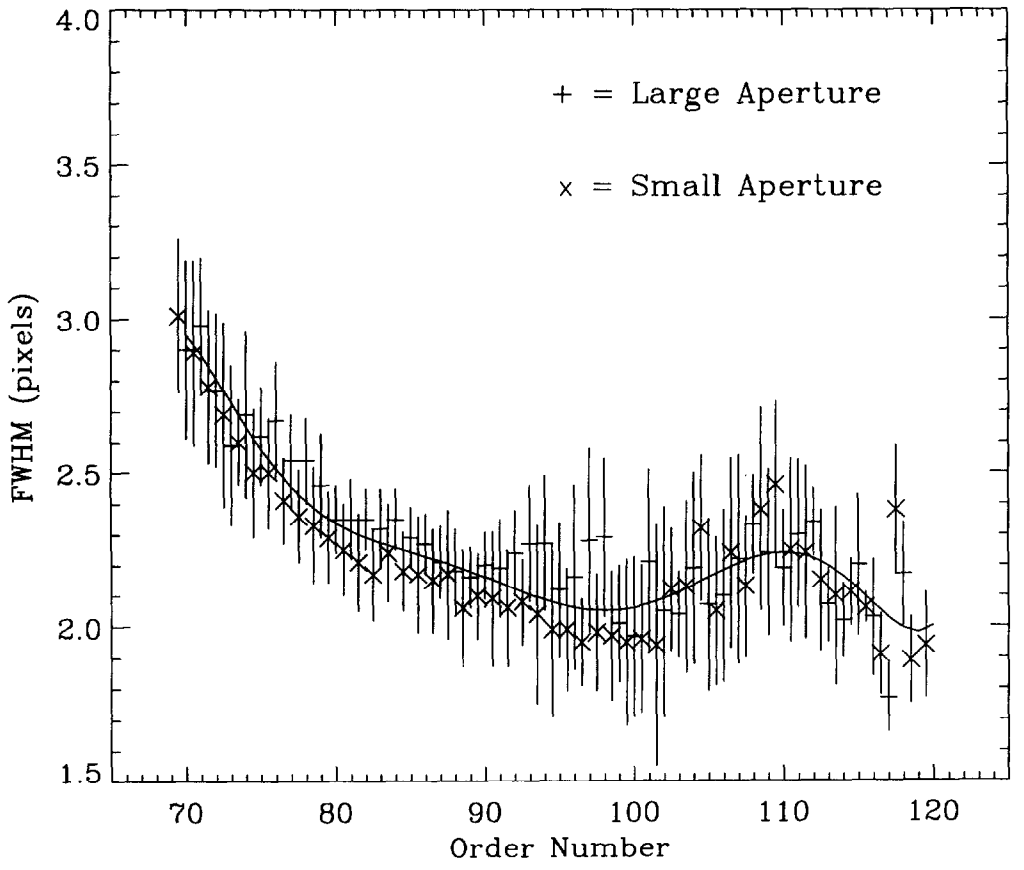

Figure 4: LWP high-dispersion spatial resolution for sample position 507. Small-aperture data is horizontally offset to the left of the large-aperture data by half an order.

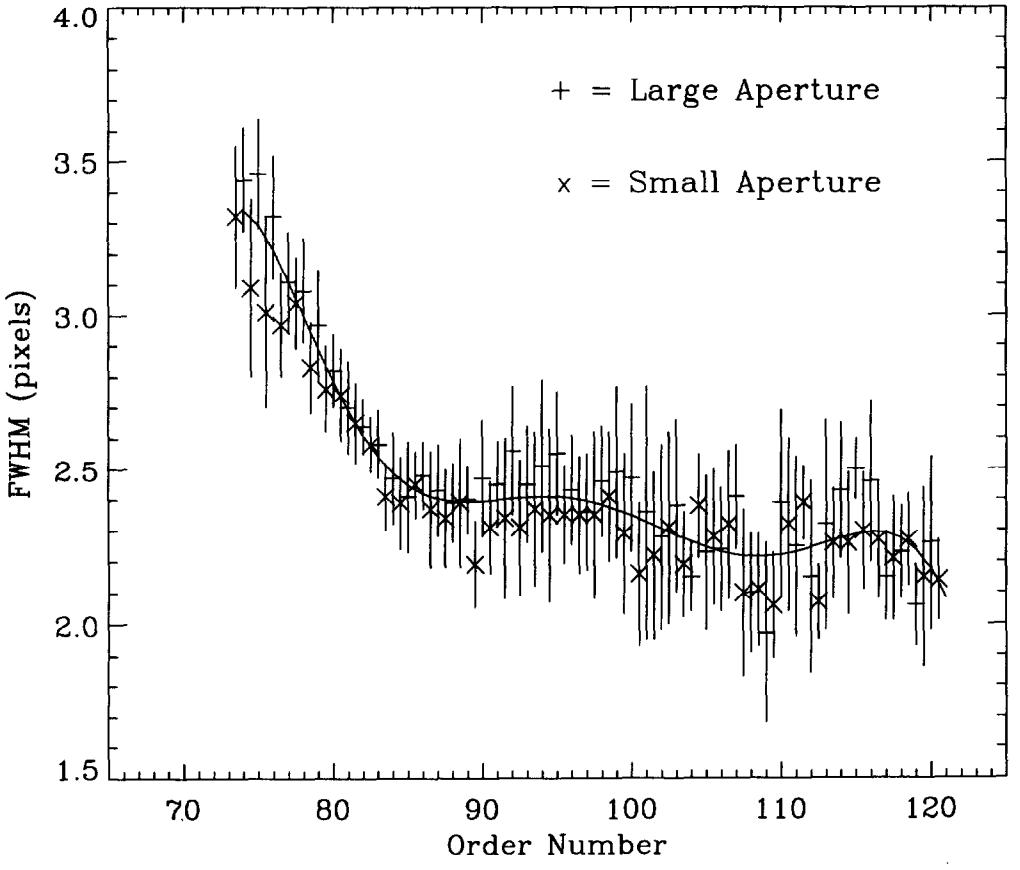

Figure 5: LWP high-dispersion spatial resolution for sample position 615. Small-aperture data is horizontally offset to the left of the large-aperture data by half an order.

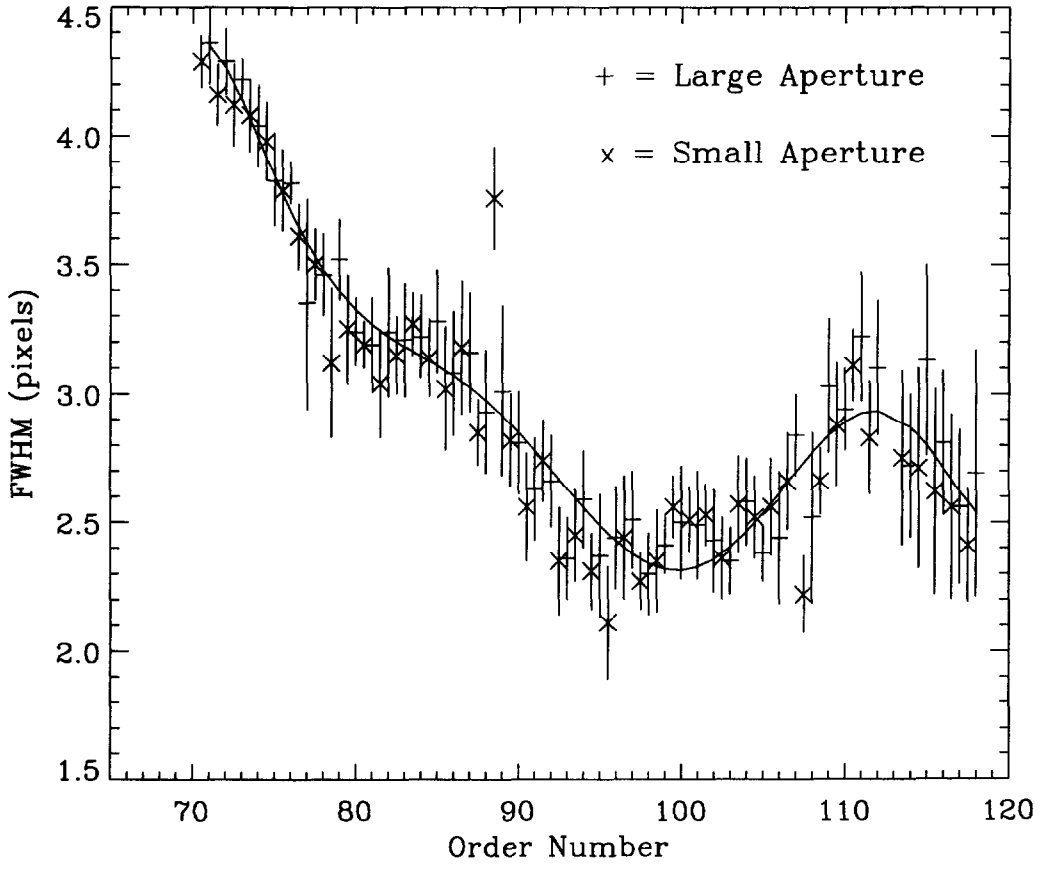

Figure 6: SWP high-dispersion spatial resolution for sample position 134. Small-aperture data is horizontally offset to the left of the large-aperture data by half an order.

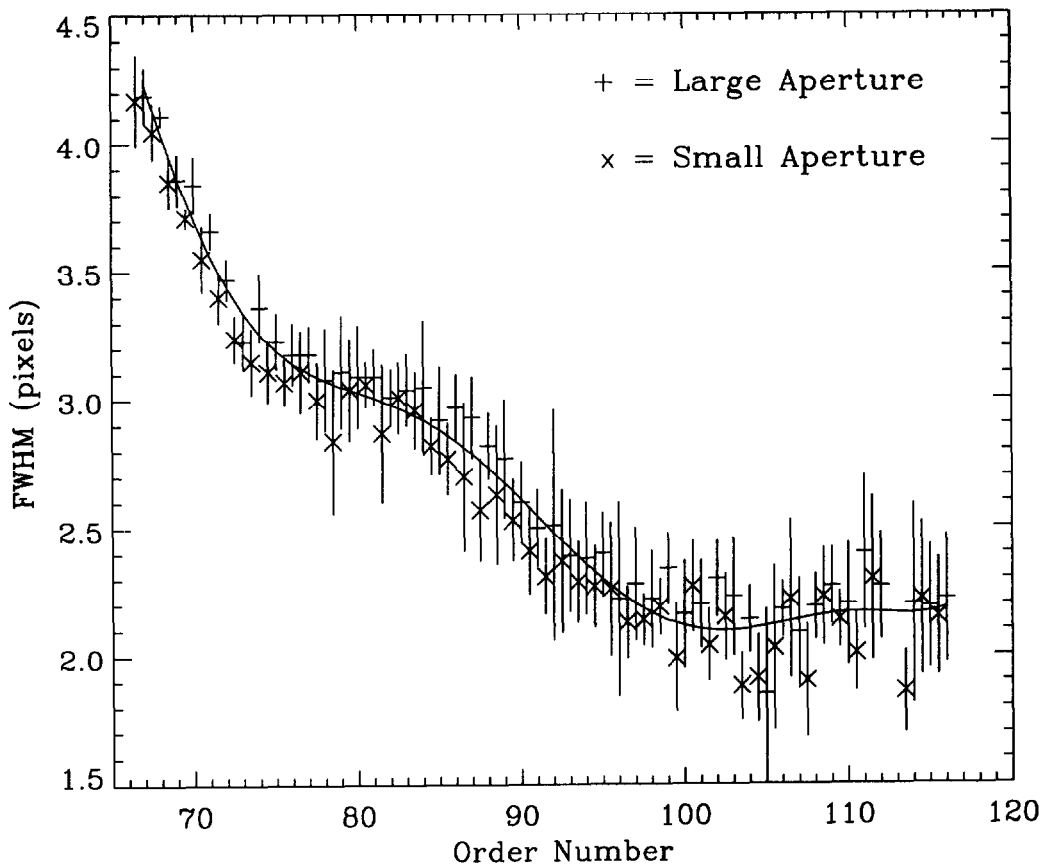

Figure 7: SWP high-dispersion spatial resolution for sample position 258. Small-aperture data is horizontally offset to the left of the large-aperture data by half an order.

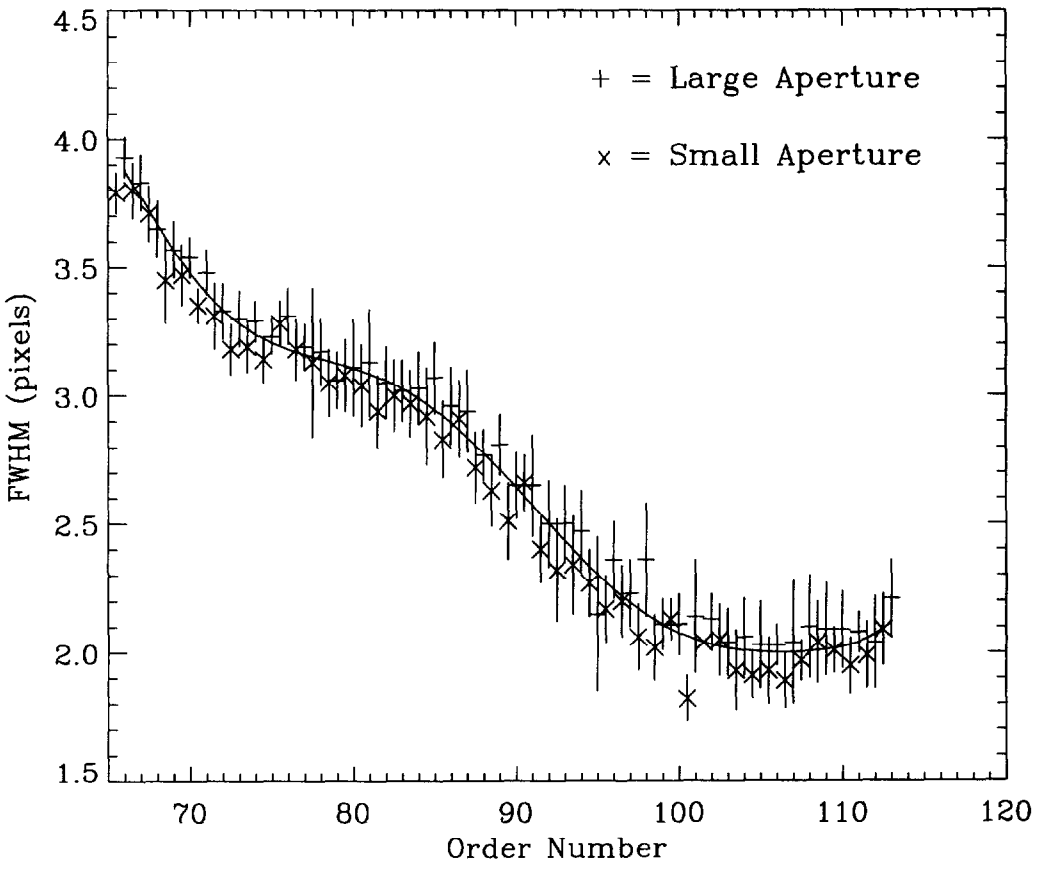

Figure 8: SWP high-dispersion spatial resolution for sample position 384. Small-aperture data is horizontally offset to the left of the large-aperture data by half an order.

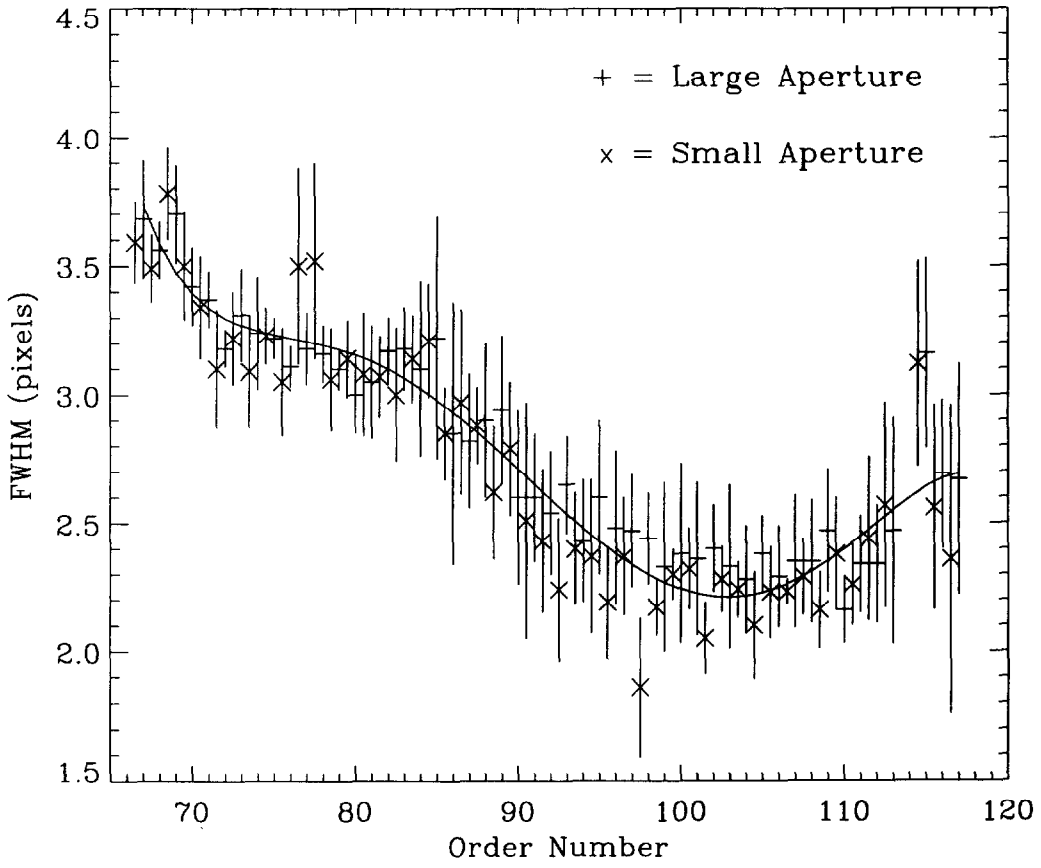

Figure 9: SWP high-dispersion spatial resolution for sample position 507. Small-aperture data is horizontally offset to the left of the large-aperture data by half an order.

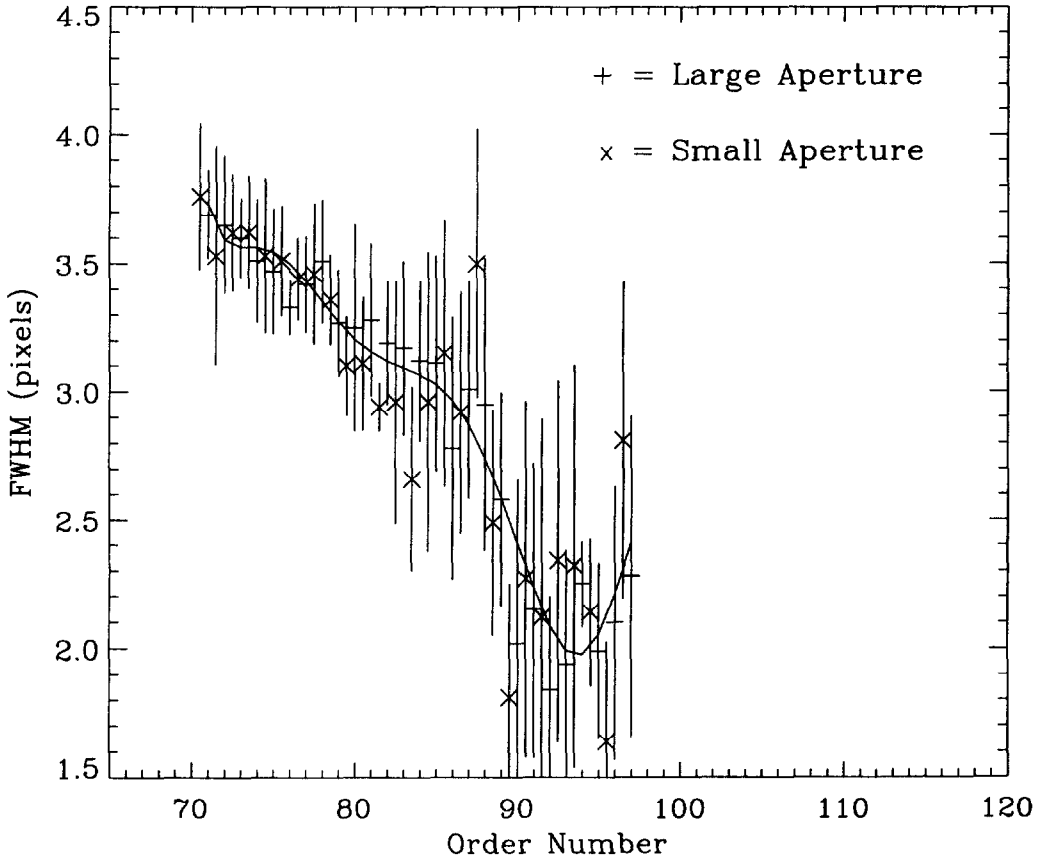

Figure 10: SWP high-dispersion spatial resolution for sample position 615. Small-aperture data is horizontally offset to the left of the large-aperture data by half an order.

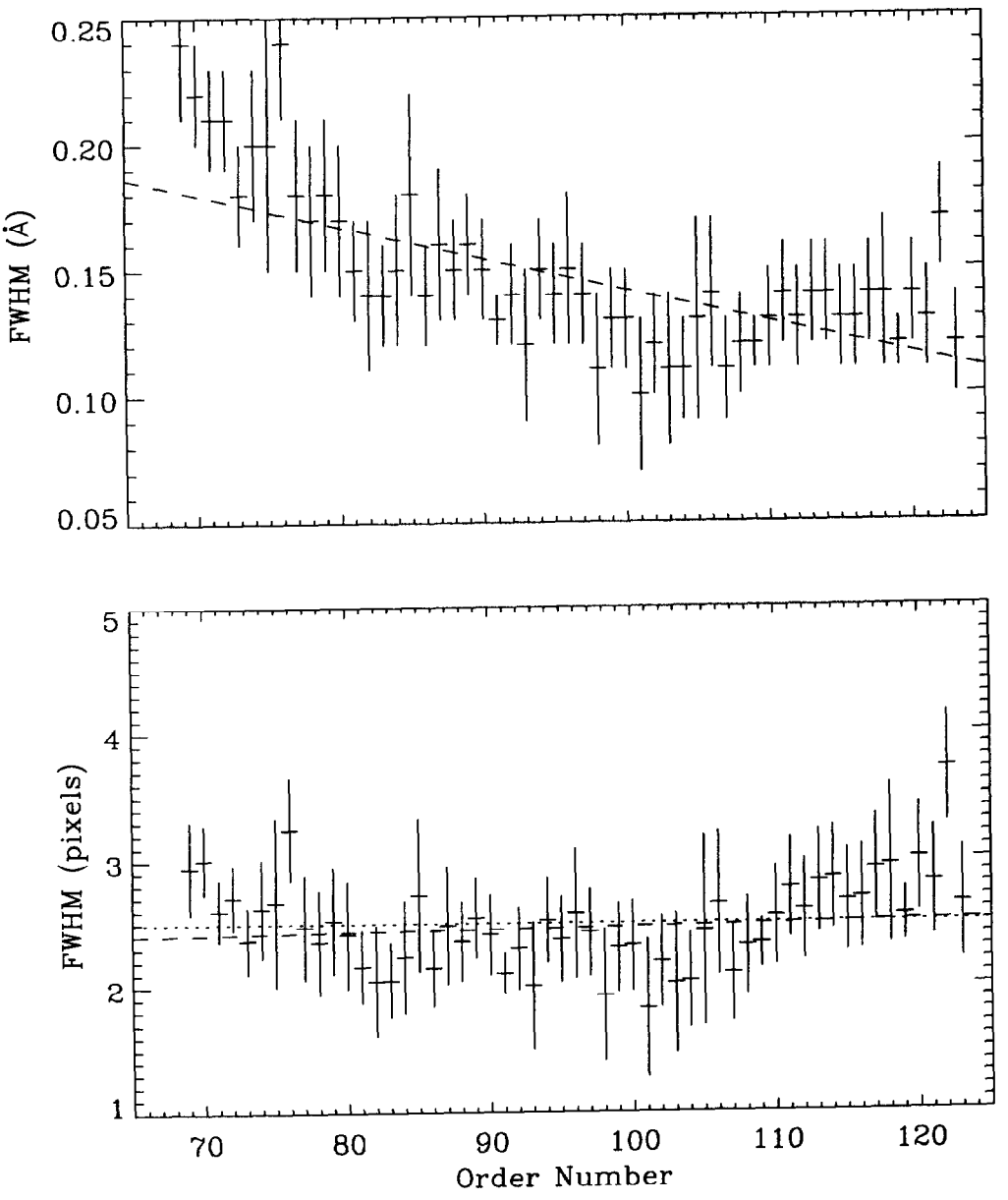

Figure 11: LWP high-dispersion spectral resolution from WAVECAL analysis.

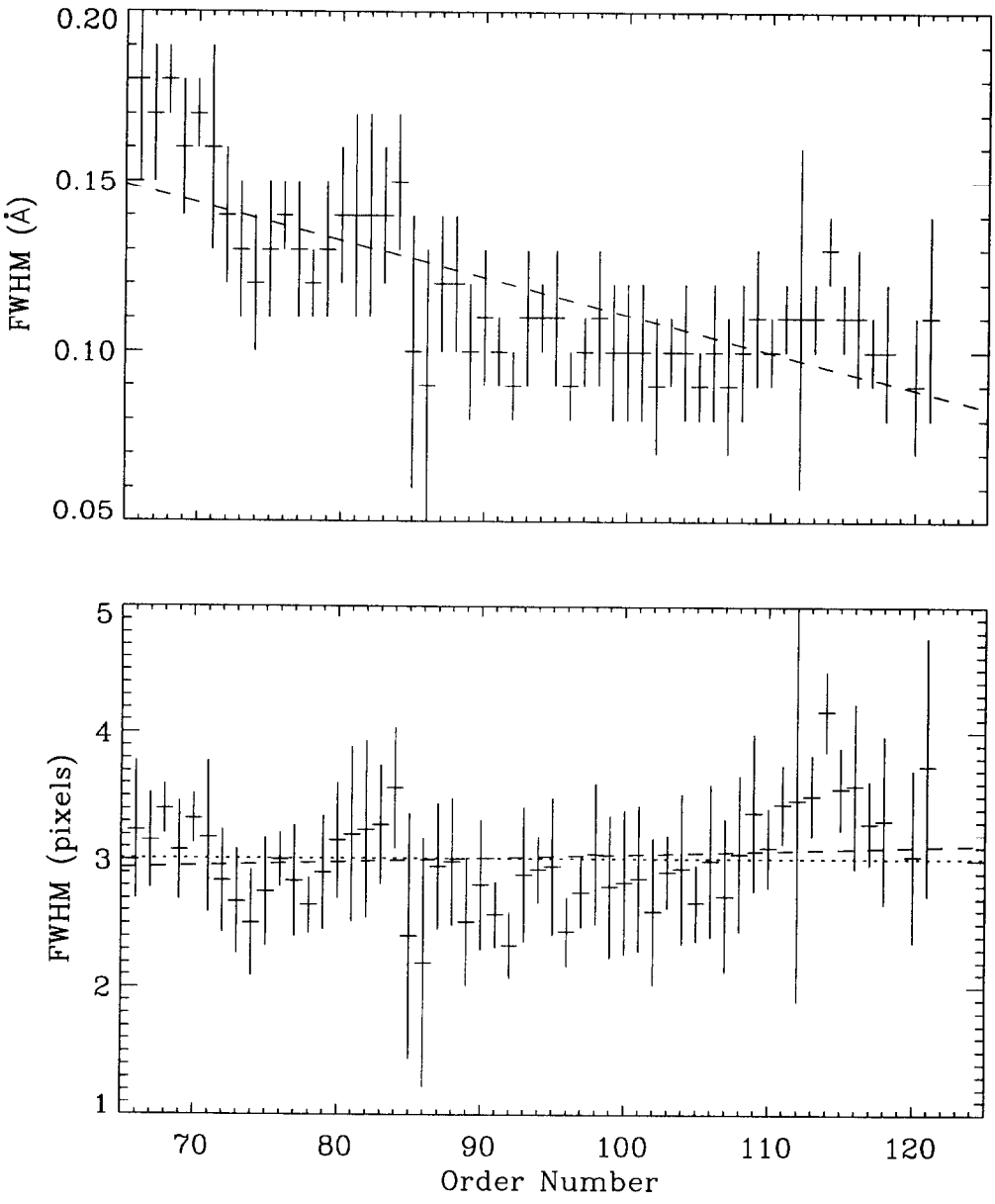

Figure 12: SWP high-dispersion spectral resolution from WAVECAL analysis.

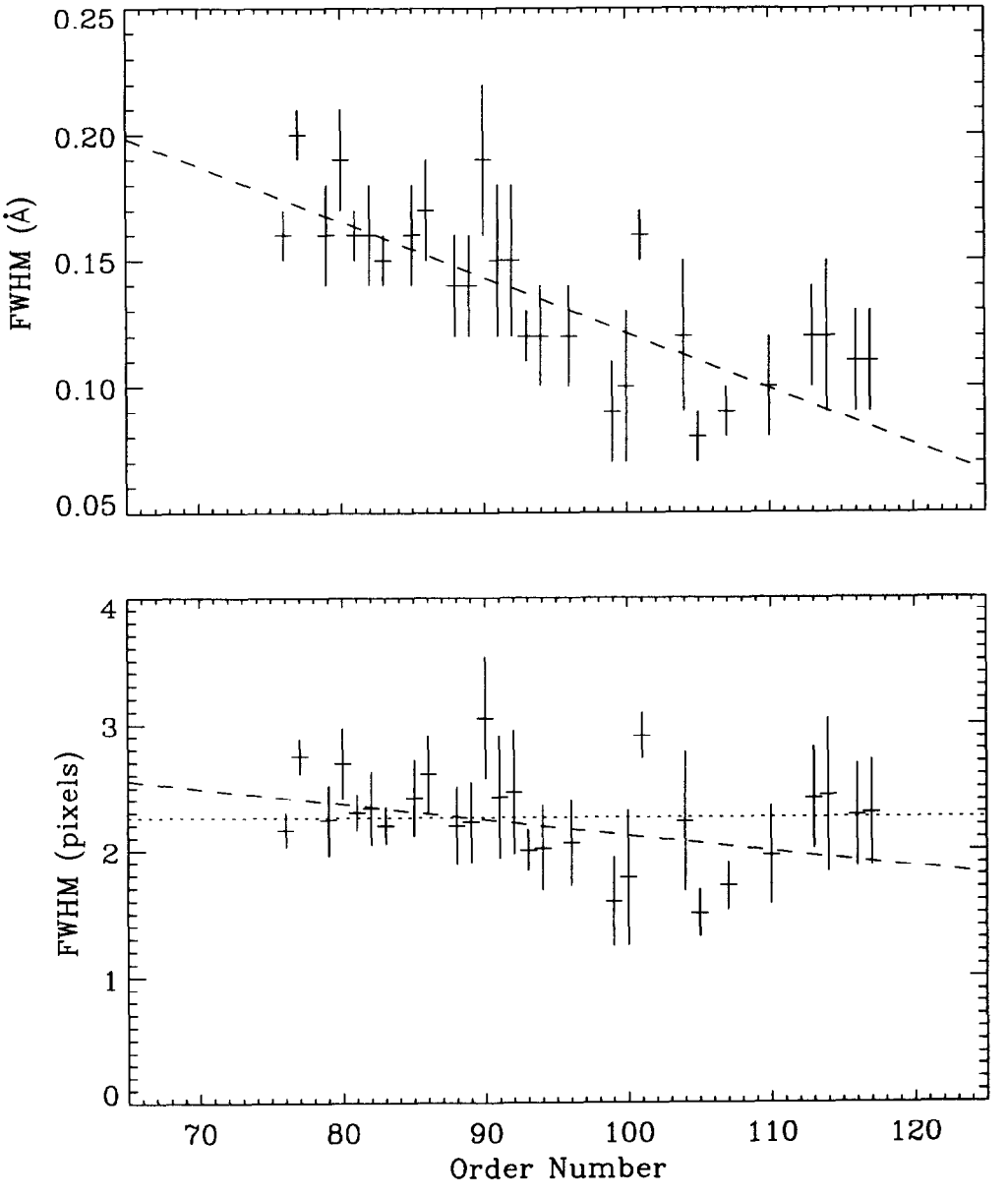

Figure 13: LWP high-dispersion spectral resolution from analysis of large-aperture Zeta Oph data.

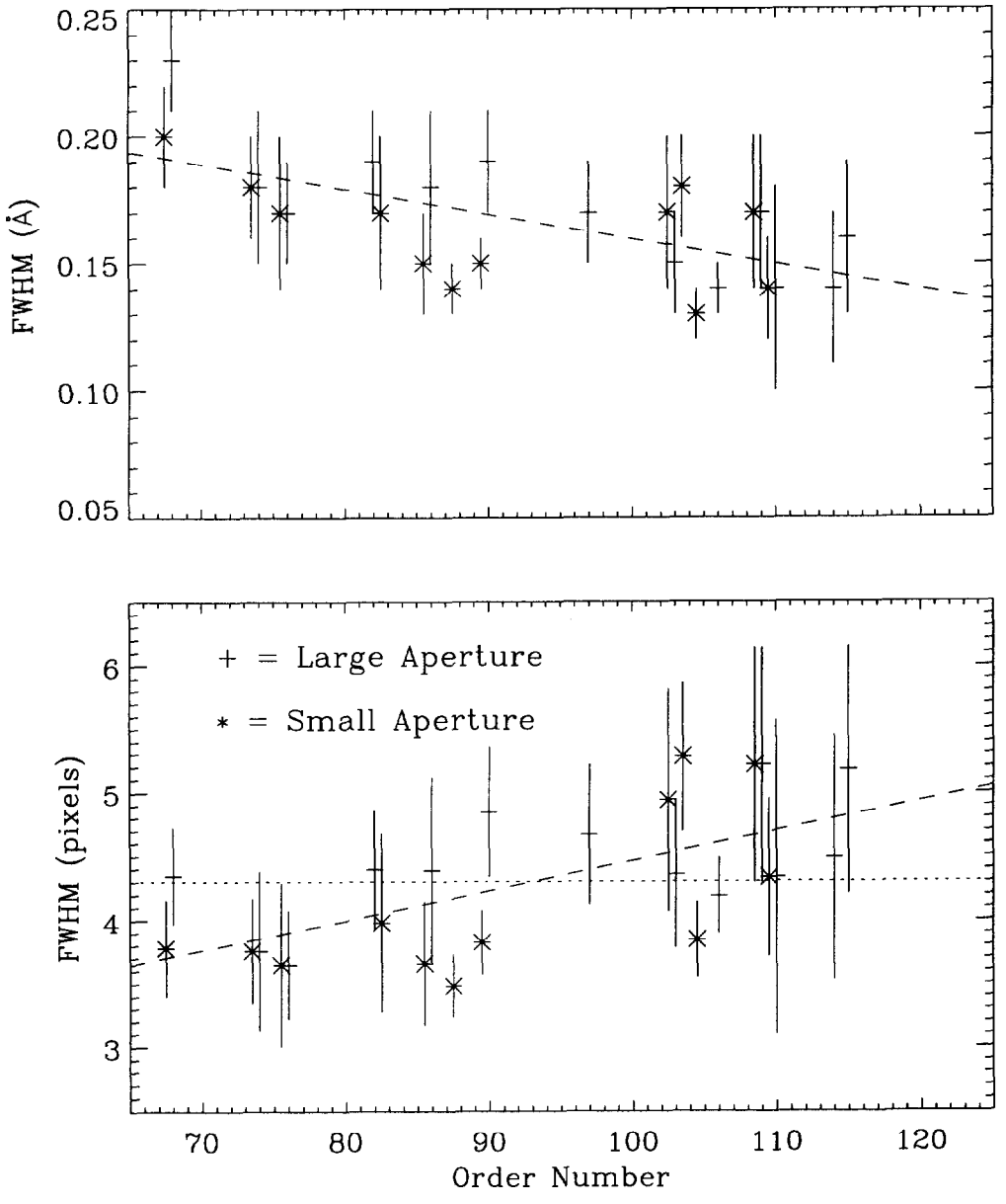

Figure 14: SWP high-dispersion spectral resolution from analysis of large- and small-aperture Zeta Oph data. Small-aperture data is horizontally offset to the left of the large-aperture data by half an order.

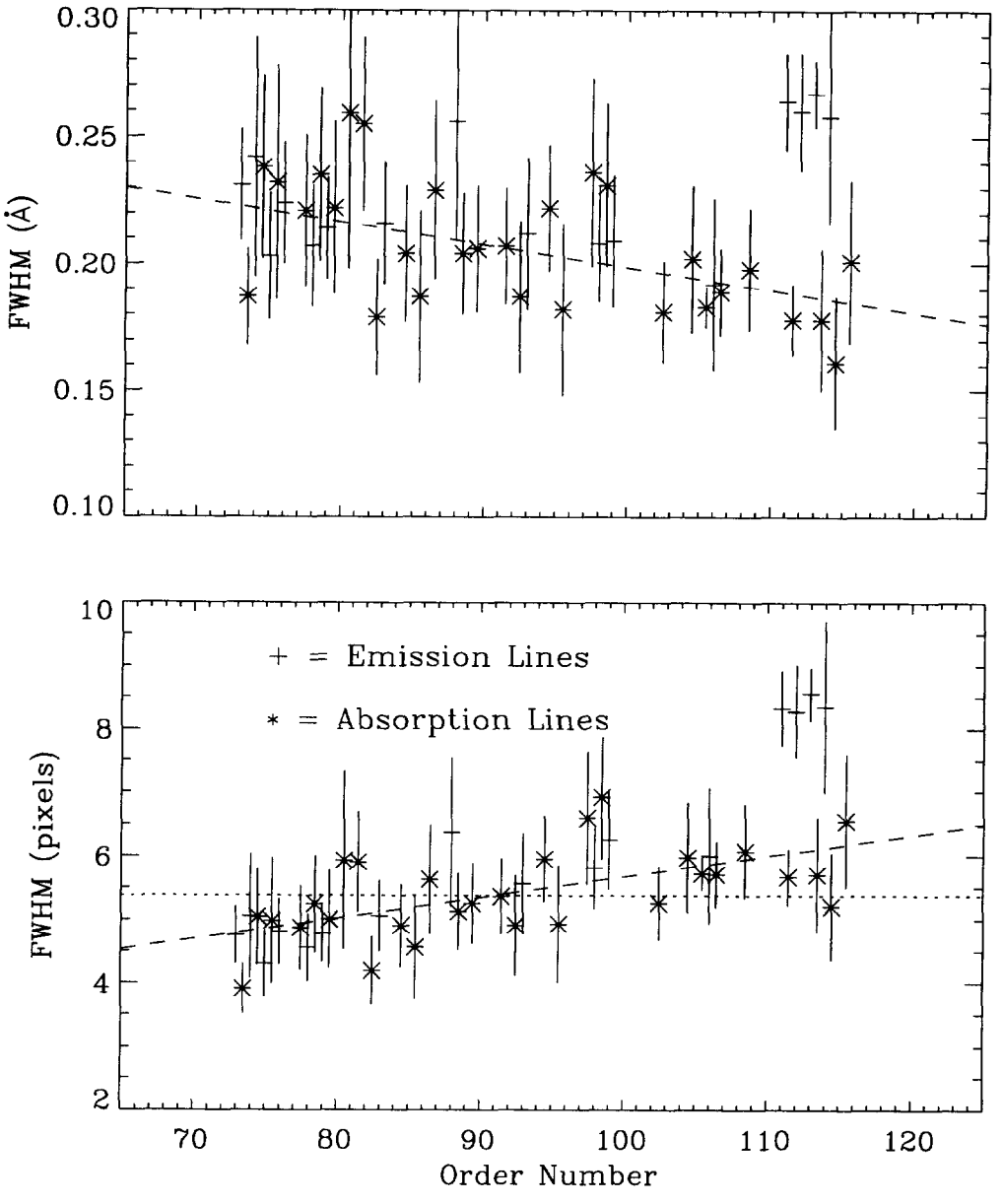

Figure 15: SWP high-dispersion spectral resolution from large-aperture stellar-source analysis. Emission line measurements for orders 111 and above were excluded from the fits. Emission line data is horizontally offset to the left of the absorption line data by half an order.

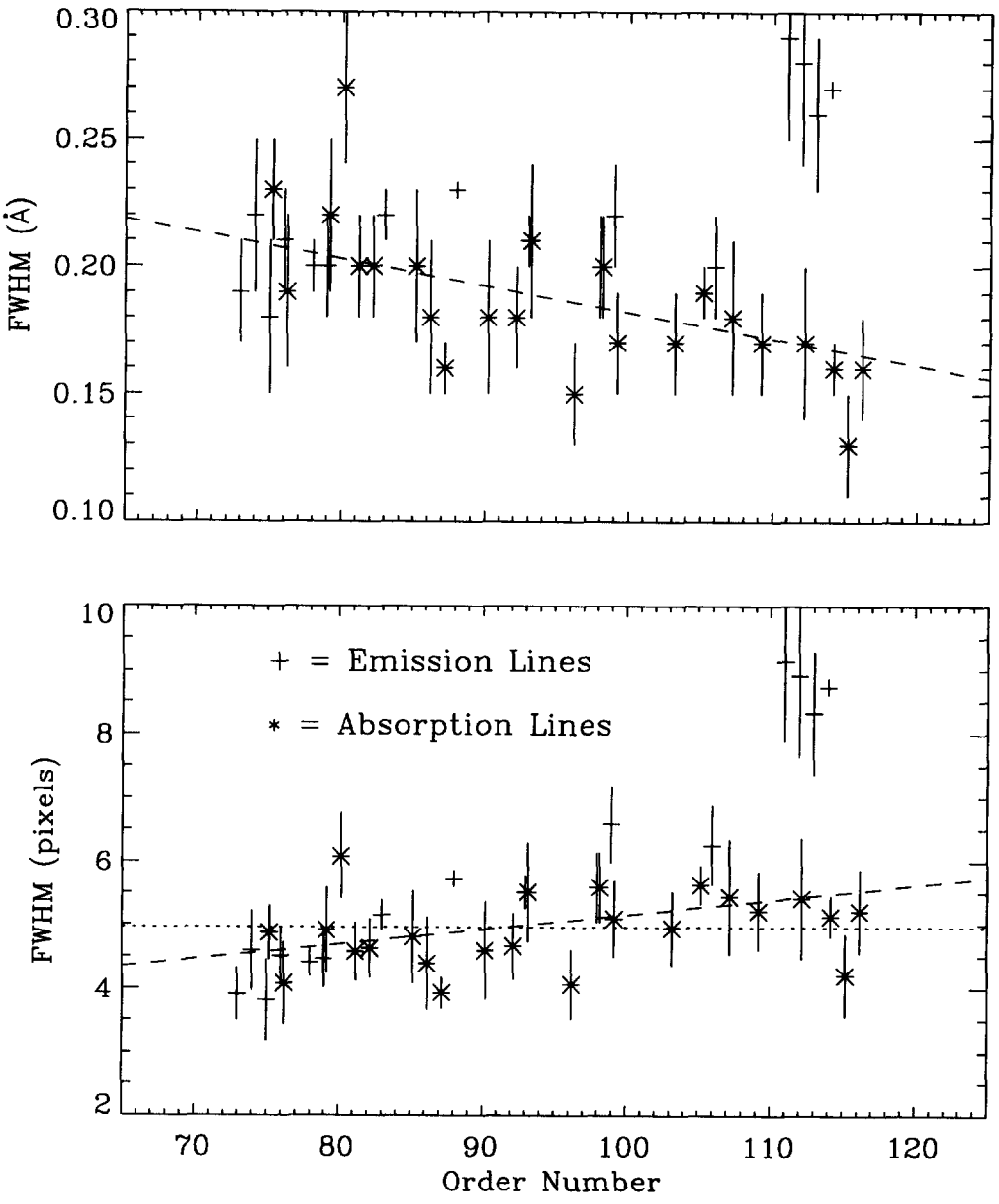

Figure 16: SWP high-dispersion spectral resolution from small-aperture stellar-source analysis. Emission line measurements for orders 111 and above were excluded from the fits. Emission line data is horizontally offset to the left of the absorption line data by half an order.